Vibrational Spectroscopy 79 (2015) 59–66

Contents lists available at ScienceDirect

Vibrational Spectroscopy

journal homepage: www.elsevier.com/locate/vibspec

Vibrational study of anharmonicity, supramolecular structure, and hydrogen bonding in two octanol isomers

S. Bauer [a,*], J. Stern [b], F. Böhm [c], C. Gainaru [a], M. Havenith [c], T. Loerting [b], R. Böhmer [a]

[a] Fakultät Physik, Technische Universität Dortmund, 44227 Dortmund, Germany
[b] Institute of Physical Chemistry, University of Innsbruck, 6020 Innsbruck, Austria
[c] Fakultät für Chemie und Biochemie, Ruhr-Universität Bochum, 44780 Bochum, Germany

ARTICLE INFO

Article history:
Received 2 February 2015
Received in revised form 22 April 2015
Accepted 4 May 2015
Available online 7 May 2015

Keywords:
Infrared
Near-infrared
Anharmonicity
Hydrogen-bonding
Monohydroxy alcohols
Structural isomers

ABSTRACT

Results from far-, mid-, and near-infrared spectroscopy are presented and combined with previous dielectric data on 2-ethyl-1-hexanol and 4-methyl-3-heptanol. This yields the electromagnetic absorption spectrum of the two monohydroxy alcohols, presented in terms of the imaginary part of the complex refractive index in a very wide frequency range. Low-frequency Raman measurements and far-infrared spectra hint at differences in the supramolecular structure of the two alcohols. By comparing the wavenumbers and amplitudes of the fundamental and the first overtone of the hydroxyl group's stretching vibration the temperature dependence of anharmonic effects and hydrogen bond cooperativity is studied.

1. Introduction

At the microscopic level hydrogen bonding can lead to a wealth of complex suprastructures that constantly break and reform. This thermally driven property governs the functionality of many bio-macromolecules. Relatively small hydrogen bonded molecules are currently under scrutiny as well, like for example sugars [1,2], pharmaceuticals [3], alcohols [4,5], and other substances of interest for the life sciences. The detailed nature of their supramolecular organization depends on the hydrogen bond strength and on molecular structure. Therefore, the study of isomeric species has been exploited for a long time using vibrational spectroscopy [6]. By focusing on the OH stretching vibration, the hydrogen-bonding partners can be accessed directly. This allows one to study the consequences of intra- and intermolecular hydrogen bonding [7,8] as well as that of hydrogen bond cooperativity [9]. The latter term refers to the observation that the addition of molecules to a hydrogen bonded network enhances the mutual bonding strength of its constituents and thus shifts the corresponding vibrational frequencies. The impact of hydrogen bond cooperativity is interesting to study in the condensed [10] as well as in the gas phase [11].

In the present work we focus on the liquid state of the isomeric octanols 2-ethyl-1-hexanol (2E1H) and 4-methyl-3-heptanol (4M3H). For the two monohydroxy alcohols previous studies inferred chain-like (in 2E1H) and ring-like (in 4M3H) supramolecular association patterns [12–19]. Here, we investigate these alcohols using far infrared (FIR), mid infrared (MIR), and near infrared (NIR) spectroscopy. To put the results for the absorption of electromagnetic radiation in perspective, we compile the dielectric spectra for the two alcohols [13,19] together with infrared results from previous [13,20] and the current study after transforming the data into a common format, the imaginary part, k, of the complex refractive index, $n^* = n - ik$. Here n designates the (real part of the) index of refraction. For nonmagnetic substances from $n^{*2} = \varepsilon^* = \varepsilon' - i\varepsilon''$ one derives $k = \left[\frac{1}{2}(\varepsilon'^2 + \varepsilon''^2)^{1/2} - \frac{1}{2}\varepsilon'\right]^{1/2}$. Using the Lambert–Beer law, $A = \varepsilon_{IR}cd = \ln(I_0/I)$, and measuring the attenuated intensity, $I = I_0\exp(-\alpha d)$, referring to the passage of a beam with intensity I_0 through a sample of thickness d, the absorption coefficient $\alpha = 4\pi k/\lambda = \varepsilon_{IR}c$ and hence k can be obtained in a straightforward manner. Here λ is the wavelength, ε_{IR} is the molar extinction coefficient, and c is the concentration of the absorbing species.

In Fig. 1 we plot k over a wide range of frequencies f. Focusing first on the low-frequency range (<0.1 THz), one recognizes that the overall shape of $k(f)$ looks similar for both alcohols. The large differences in the amplitudes of k for the two alcohols are due to

* Corresponding author. Tel.: +49 231 755/3560; fax: +49 231 755/3516.
E-mail address: stefanb@e3.physik.tu-dortmund.de (S. Bauer).

http://dx.doi.org/10.1016/j.vibspec.2015.05.001
0924-2031/

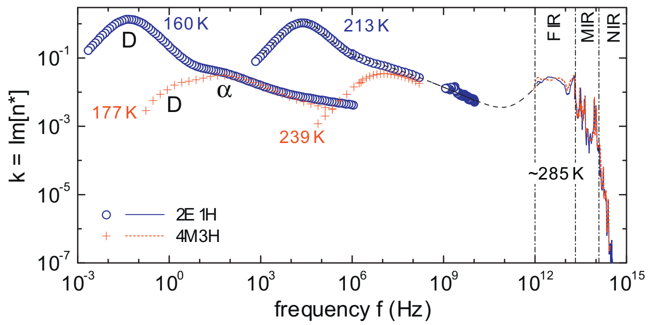

Fig. 1. Temperature dependence of the imaginary part, k, of the complex index of refraction n^* for 2E1H and 4M3H comprising the frequency range below about 0.1 THz in which effects of orientational polarization dominate. Structural (α) and Debye (D) relaxation peaks are marked for the low-temperature spectra. The dashed line is drawn to guide the eye. Infrared data are also represented in terms of k for the two alcohols at $T \approx 285$ K. The vertical dashed–dotted lines separate the frequency intervals typically associated with the FIR, MIR, and NIR spectral ranges.

the effective addition of the molecular dipole moments if chain-like patterns prevail, like for 2E1H, or their near cancelation in ring-like supramolecular structures, like for 4M3H. Yet in the representation of Fig. 1 the spectra of the two monohydroxy alcohols look rather similar in the THz regime. Therefore, it is one of the goals of the present work to examine the impact of the different supramolecular structures of the two alcohol isomers on their infrared spectra in more detail.

First, we will present MIR data in the regime of the OH group's fundamental stretching vibration with the associated wavenumbers designated as $\overline{\nu}^{(1)}$. Consequently, the wavenumbers of the corresponding first overtone, appearing in the NIR spectral region, will be labeled as $\overline{\nu}^{(2)}$. The observation of overtones is per se an indication for anharmonicity, since overtones do not occur in a perfectly harmonic potential. Therefore, by comparing $\overline{\nu}^{(1)}$ and $\overline{\nu}^{(2)}$ the extent of anharmonicity may be inferred [21]. One usually distinguishes (i) so-called mechanical anharmonicity, referring to deviation from a parabolic shape of the vibrational potential and (ii) so-called electrical anharmonicity. The latter arises if the transition dipole moment changes non-linearly along its vibrational coordinate, see, e.g., [22]. While in studies of liquids the two contributions are often difficult to disentangle experimentally, in principle they should be considered separately, since they can either add up or at least partially compensate each other [23]. Furthermore, anharmonic effects are typically affected by the strength of hydrogen bonding [11,24,25] and by coupling of modes [26].

Finally, the FIR absorption and the Raman scattering of 2E1H and 4M3H are studied for wavenumbers up to about 650 cm^{-1} with an interest in exploring whether and how the intermolecular stretching vibration, ν_σ(O···H), along a hydrogen bond connecting two or more molecules reflects the different supramolecular structures of the two octanol isomers. Recently, a number of investigations on monohydroxy alcohols have focused on the difficult-to-access THz regime [27–29]. Nevertheless, while data on various alcohols have been published earlier, see, e.g., [30,31], FIR spectra for isomeric octanols are apparently not available.

2. Experimental details

The monohydroxy alcohol samples were purchased from Sigma–Aldrich with stated purities of ≥99% for 2E1H as well as for 4M3H (mixture of erythro and threo isomers) and used without further treatment.

The MIR measurements were conducted using a Varian Excalibur 3100 FT-IR spectrometer with a resolution of 4 cm^{-1}. Three droplets about 2 mm in diameter were dispersed between two optical AgCl windows with a diameter of 25 mm. This resulted in a film of about 10–30 μm thickness. The windows were fixed onto a cryogenic sample holder and inserted into a vacuum chamber that was pumped to a base-pressure of ~10^{-2} mbar. Two optical KBr windows of 49 mm diameter allowed the beam of light to pass through chamber and sample. The temperature was measured by a Pt100 sensor located at a distance of about 1 cm from the optical windows. The MIR spectra were corrected by subtracting a constant background, determined in the wavenumber range from 2200 to 2350 cm^{-1} in which no significant absorbance occurs [32,33]. Then, the spectra were normalized by the CH peak intensity at 2874 cm^{-1} in the 270 K spectrum. The analyzed NIR data were taken from previous work [13,20].

FIR measurements were performed using a Bruker Vertex 80v FT-IR spectrometer with a liquid helium cooled silicon bolometer detector from Infrared Laboratories. The monohydroxy alcohols were placed in a Bruker liquid cell with polycrystalline diamond windows of 500 μm thickness separated by a 208 μm thick polyethylene spacer. The temperature of the cell was kept constant at 293 K with a thermostat. The sample chamber was purged with dry nitrogen before and during measurement to reduce air humidity. For each spectrum 256 scans with a maximum resolution of 2 cm^{-1} were averaged and then a sliding average of 25 data points was applied to minimize etalon (standing wave) effects.

Raman measurements were performed using an alpha 300 R/A/S confocal Raman microscope from WITec with a frequency-doubled Nd:YAG laser of 532 nm wavelength as excitation source. The excitation beam was coupled into the microscope with a single-mode optical fiber and focused onto the liquid sample with a 20× objective (numerical aperture = 0.4). In a 180° geometry the Raman scattered light was collected by the same objective. Via a multimode fiber of 50 μm diameter and a diffraction grating of 1800 grooves/mm the light was directed onto a back-illuminated electron multiplying charge-coupled device detector (200 × 1600 pixels, cooled to –60 °C). For each sample 5 spectra with an integration time of 20 s and a spectral resolution of <1 cm^{-1} were averaged.

3. Results and analysis

3.1. Mid-infrared spectroscopy

In Fig. 2(a) and (c) we present temperature dependent MIR spectra of 2E1H and 4M3H, respectively, in the wavenumber range from 3000 to 3700 cm^{-1} corresponding to the region of the fundamental OH stretching vibration ν(OH) [32,34]. A broad absorbance band appears in this spectral range around ~3300 cm^{-1} that can be decomposed [34–36] into bands arising from strongly hydrogen bonded OH species conventionally designated [37] as δ state and from weakly bonded proton donating hydroxyl groups labeled γ state. The absorbance of the γ state is small compared to that of the δ state and becomes noticeable only as an asymmetrically broadened high-wavenumber flank of the δ band. The absorbance of free OH groups (α state) as well as that of weakly hydrogen bonded proton accepting hydroxyl groups (β state), strongly overlaps and usually a single absorbance band is found at wavenumbers close to 3630 cm^{-1} [34,38,39]. Below room temperature the α/β band is very faint indicating that only a small number of non- or weakly bonded OH groups exist.

Clear spectral changes emerge upon cooling the monohydroxy alcohols. Let us first turn to the δ band positions, $\overline{\nu}_\delta^{(1)}$, that we have read off from the absorbance maxima of the data in Fig. 2(a) and (c). The results are presented in Fig. 3. For both

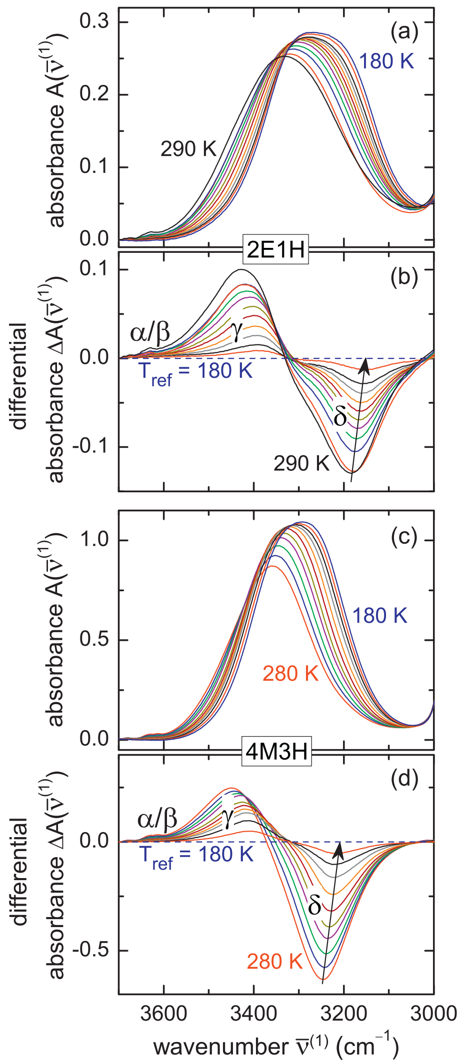

Fig. 2. MIR data recorded in steps of 10 K for a wide range of temperatures: the panels show (a) absorbance and (b) difference spectra of 2E1H as well as (c) absorbance and (d) difference spectra of 4M3H. The arrows highlight the temperature dependent red shift of the differential absorbance of the δ band for each alcohol. The ~4 times larger intensity for 4M3H results from an increased path length.

alcohols one recognizes an approximately linear red shift of $\overline{\nu}_\delta^{(1)}$ with decreasing temperature. Then, Fig. 4(a) shows that the maximum absorbance of the δ state, $A(\overline{\nu}_\delta^{(1)})$, read off at the peak position $\overline{\nu}_\delta^{(1)}(T)$ increases non-linearly with decreasing temperature: at $T \sim 250$ K a kink in $A(\overline{\nu}_\delta^{(1)})$ is seen for 2E1H and for 4M3H. This "250 K anomaly" was already found in the NIR spectra of several monohydroxy alcohols including 2E1H and 4M3H. It was interpreted in terms of a redistribution among different hydrogen bonded suprastructures partaking in a temperature dependent equilibrium [20,40,41].

To examine the temperature dependence of the spectral shapes from a slightly different perspective we calculated difference spectra, $\Delta A(\overline{\nu}^{(1)}, T) = A(\overline{\nu}^{(1)}, T) - A(\overline{\nu}^{(1)}, T_{ref})$ with T_{ref} = 180 K (see Fig. 2(b) and (d)). Three bands appear in $A(\overline{\nu}^{(1)}, T)$ upon heating the samples: a loss peak, $\Delta A(\overline{\nu}_\delta^{(1)})$, that is associated with the δ state, a gain peak, $\Delta A(\overline{\nu}_\gamma^{(1)})$, due to the γ state, and another small gain peak, $\Delta A(\overline{\nu}_{\alpha/\beta}^{(1)})$, caused by α/β oscillators. The spectral positions of the various bands are summarized in Table 1. The temperature

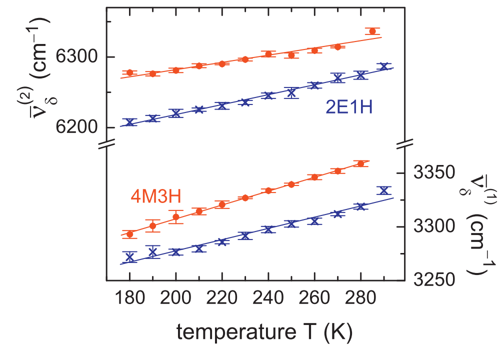

Fig. 3. Temperature dependence of the δ band peak position in the MIR, $\overline{\nu}_\delta^{(1)}$, as well as in the NIR spectral region, $\overline{\nu}_\delta^{(2)}$, for the two octanol isomers 4M3H and 2E1H. The peak wavenumbers are read off from the absorbance maxima of the δ bands presented in Fig. 2(a) and (c) as well as in Refs. [13] and [20]. Error bars represent the experimental uncertainty in the peak positions due to broadened bands. (For an interpretation of the references to color in the text, the reader is referred to the web version of this article.)

dependences of $\Delta A(\overline{\nu}_\delta^{(1)})$ and $\Delta A(\overline{\nu}_\gamma^{(1)})$ are presented in Fig. 4(b). With increasing temperature $\Delta A(\overline{\nu}_\gamma^{(1)})$ becomes more intense indicating that the number of weakly bonded proton donating OH groups increases.

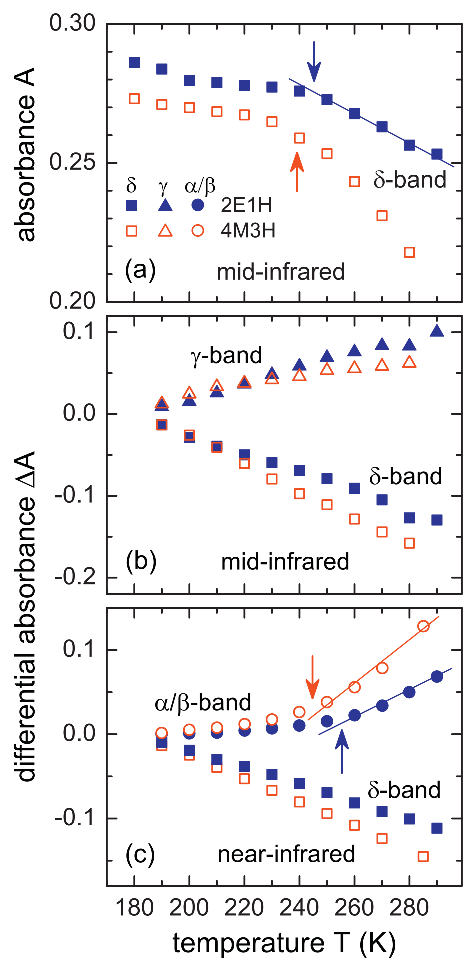

Fig. 4. Temperature dependence of (a) the MIR δ band absorbance, (b) the MIR differential absorbance amplitudes, and (c) the NIR differential absorbance amplitudes. The lines and arrows emphasize that for several quantities the temperature evolution of the absorbance changes below about 250 K. Note that for 4M3H the MIR band absorbances are divided by four to facilitate comparison with the data for 2E1H.

Table 1
Peak wavenumbers (in cm^{-1}) of several OH oscillator states taken from the mid- and near-infrared difference spectra of the isomeric octanols 2E1H and 4M3H recorded at 270 K. The existence of two absorbance maxima for the NIR α/β band of 4M3H shows that the α and β oscillator states are in fact separated.

	2E1H	4M3H
$\overline{\nu}_{\delta}^{(1)}$	3176	3242
$\overline{\nu}_{\gamma}^{(1)}$	3420	3445
$\overline{\nu}_{\alpha/\beta}^{(1)}$	3630	3630
$\overline{\nu}_{\delta}^{(2)}$	6175	6216
$\overline{\nu}_{\gamma}^{(2)}$	6760	6810
$\overline{\nu}_{\alpha/\beta}^{(2)}$	7098	7097/7063

In the supercooled liquid 2E1H linear supramolecular structures were reported to prevail [12–14]. The terminal γ state appears only once in each aggregate and hence it can be regarded to count the number of H-bonded 2E1H chains. Thus, from the increase in $\Delta A(\overline{\nu}_{\gamma}^{(1)})$ we conclude that upon heating this number increases. Since simultaneously the differential δ band absorbance decreases upon heating the sample, see Fig. 4(b), the main effect of increased temperature is a shortening of the chains.

Although the (differential) MIR spectra for 2E1H and 4M3H look similar, see Fig. 2, and the thermal evolution of the peak absorbances is analogous, see Fig. 4(b), the arguments just made cannot be applied to 4M3H directly. This is because from techniques such as nuclear magnetic resonance [19], dielectric spectroscopy [15,42], and X-ray scattering [43] it has been suggested that ring-like or cyclic supramolecular structures dominate in 4M3H. In ring-forming systems, the absorbance of the γ state just reflects any weakly bonded terminal OH groups. Note that the existence of branched supramolecular H-bonded aggregates has been neglected in this discussion. From Monte Carlo simulations it is evident that these structures coexist with linear or ring-like clusters [44]. Taken together this suggests that MIR spectroscopy is not fully suited to distinguish the different suprastructures in the two octanol isomers. However, such a distinction becomes possible, at least close to room temperature, by analyzing the absorption bands of various H-bonded aggregates in the overtone region.

3.2. Overtone spectroscopy

In first overtone vibrational spectra of monohydroxy alcohols a number of essentially temperature independent CH combination bands are present [45] between 7400 and 6900 cm^{-1} and several bands strongly overlap. Therefore, NIR *difference* spectra are particularly useful to study temperature induced spectral changes. In Fig. 5 we present the differential absorbance, $\Delta A(\overline{\nu}^{(2)})$, for (a) 2E1H and (b) 4M3H as calculated from the data of Refs. [13] and [20], respectively. Near 7100 cm^{-1}, a gain peak emerges with increasing temperature that includes contributions from free or proton donating terminal OH groups (α/β band). For 4M3H, this absorbance maximum exhibits a low-wavenumber shoulder which reflects equally populated α and β oscillator states, in accordance with 2D near-infrared spectroscopic studies of several sterically hindered monohydroxy alcohols [46]. This suggests the occurrence of a large number of small aggregates at room temperature. The broad gain peak near 6770 cm^{-1} in the spectrum of 2E1H and near 6840 cm^{-1} for 4M3H, respectively, that we term π band, is usually ascribed to (cyclic) dimers [47–50] and in general reflects the absorbance of non-cooperatively hydrogen bonded OH groups in small

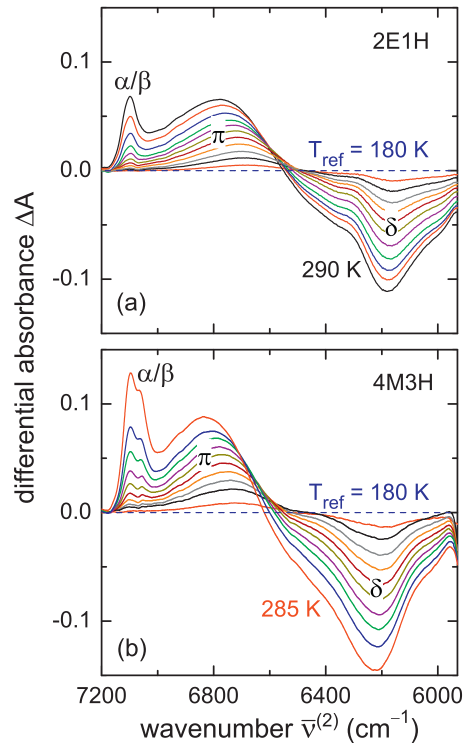

Fig. 5. Temperature dependent NIR difference spectra of (a) 2E1H and (b) 4M3H as calculated from data in Refs. [13] and [20], respectively. The data were taken in steps of 10 K except for the highest temperature of 4M3H. For both samples a reference temperature of 180 K was chosen. Various bands are labeled using Greek letters. Indications for γ bands (near 1430 nm) are not obvious in this representation.

aggregates. The faint signature of the γ band visible in the NIR and MIR spectra partially overlaps with the π band absorbance but cannot be resolved unambiguously in the NIR difference spectra.

The temperature dependence of the peak absorbances for the δ loss peak, $\Delta A(\overline{\nu}_{\delta}^{(2)})$, and for the α/β gain peak, $\Delta A(\overline{\nu}_{\alpha/\beta}^{(2)})$, presented in Fig. 4(c) shows similar trends as in the fundamental region. The absorbance of the α/β NIR bands displays an enhanced absorbance gain for $T \geq 250$ K confirming findings for several other monohydroxy alcohols [20]. In Section 3.1 we concluded that with increasing temperature a disintegration of chain-like H-bonded structures into monomers or smaller aggregates occurs for 2E1H. Now from the appearance of the π band it becomes clear that the latter are mostly (cyclic) dimers. To quantify the relative number of monomers, dimers, and higher multimers knowledge about their molar extinction coefficient, ε_{IR}, is required. An experimental access to molar extinction coefficients is often provided by variation of the alcohol concentration, see for example [51].

According to Walrafen et al. [52] an estimate is possible for the ratio $m = \varepsilon_{IR,b}/\varepsilon_{IR,nb}$ of molar extinction coefficients which here refers to bonded and non-bonded (or weakly bonded) species. Based upon NIR difference spectra this ratio can be obtained by plotting the absolute value of the integrated absorbance loss, $|L|$, versus the integrated absorbance gain, G. The evaluation of the slope $\Delta L/\Delta G$ in such a plot yields m. For both monohydroxy alcohols we find a linear $L(G)$-dependence (not shown) with a slope $m \approx 1.4$. This implies that the NIR absorption cross section of an H-bonded hydroxyl group is about 40% larger than that of weakly or non-bonded OH species. In the fundamental region, the $\Delta L/\Delta G$ ratio shows a non-linear temperature dependence that impedes a precise determination of m.

3.3. Anharmonicity

In the entire temperature range investigated the δ bands of 4M3H appear blue shifted compared to those of 2E1H (see Fig. 3). Interpreted in terms of a harmonic oscillator, $\overline{\nu} \propto \sqrt{K/m_r}$, and assuming the same reduced mass m_r for the hydroxyl group of the two monohydroxy alcohols one has to conclude that the force constant K of the covalent OH bond in 4M3H is larger than that in 2E1H. Two important factors which in principle can affect the strength of the covalent OH bond are the anharmonicity of the vibrational potential, see Section 4, and whether the OH group is involved in hydrogen bonding [23,53]. In 2E1H a large number of linear clusters with essentially unstrained hydrogen bonds exist which favor a pronounced cooperativity yielding an increase of the hydrogen bond strength. Conversely, 4M3H clusters exhibit more strained, hence weakened hydrogen bonds and stronger covalent OH bonds. Thus, for 4M3H the force constants K are expected to be larger and the vibration bands appear blue shifted with respect to those of 2E1H in accordance with experiment.

Overall, with decreasing temperature the δ bands in the MIR and in the NIR regions shift linearly to the red. Apart from minor variations arising from macroscopic density changes this thermally induced red shift can be attributed to the fortification of hydrogen bonds, i.e., the average O···O distance becomes shorter upon cooling, a finding typical for monohydroxy alcohols [9,20,53,54]. The wavenumber change per Kelvin, $\Delta\overline{\nu}_\delta^{(1),(2)}/\Delta T$, is ~0.6 cm^{-1}/K for 2E1H as well as for 4M3H, cf. the arrows in Fig. 2(b) and (d). These values are comparable to those for 2-propanol ($\Delta\overline{\nu}_\delta^{(1),(2)}/\Delta T = 0.59$ cm^{-1}/K) and for tert-butanol ($\Delta\overline{\nu}_\delta^{(1),(2)}/\Delta T = 0.44$ cm^{-1}/K) [53].

Within a second-order perturbation approach the vibrational potential for bonded hydroxyl groups can be characterized by the anharmonicity constant [23,55]

$$\chi_\delta = \frac{\overline{\nu}_\delta^{(2)}}{2} - \overline{\nu}_\delta^{(1)}. \qquad (1)$$

Above about 210 K we find that $\chi_{\delta,2E1H} > \chi_{\delta,4M3H}$, cf. Fig. 6, but toward lower temperatures this behavior tends to change since $-\Delta\chi_{\delta,2E1H}/\Delta T = (0.17 \pm 0.03)$cm^{-1}/K and $-\Delta\chi_{\delta,4M3H}/\Delta T = (0.41 \pm 0.02)$cm^{-1}/K differ widely for the two octanol isomers. One also can use differential δ band positions, see Fig. 2(b) and (d), to calculate $\Delta\chi_\delta/\Delta T$. For reference temperatures of T_{ref} = 180 and 280 K we find that $-\Delta\chi_\delta^{180}/\Delta T$ and $-\Delta\chi_\delta^{280}/\Delta T$ agree with $-\Delta\chi_\delta/\Delta T$ within experimental uncertainty (not shown). Fig. 6 also includes temperature dependent anharmonicity constants of 2-propanol and tert-butanol from Ref. [53].

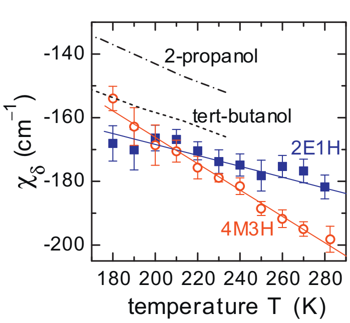

Fig. 6. Temperature dependence of the anharmonicity constant χ_δ for 2E1H and 4M3H (both from this work) as well as for 2-propanol (dash–dotted line, Ref. [53]) and for tert-butanol (dashed line, Ref. [53]). Straight lines are fits to the data. An average value of 282.5 K was used to represent the 4M3H data at the highest temperature.

So far, we have focused on the temperature dependent frequency and anharmonicity shifts related to the stretching vibrations of hydrogen *bonded* hydroxyl groups. Let us now direct attention to the free OH groups in order to assess the impact of hydrogen bonding on their anharmonicity. Like for several other alcohols [20] the wavenumbers of the MIR (Fig. 2) and NIR (Fig. 5) α/β bands of 2E1H and 4M3H are seen to be largely temperature independent. Therefore, it suffices to focus on the high-temperature spectra for which the α/β bands at $\overline{\nu}_{\alpha/\beta}^{(1),(2)}$ show large absorbances. For 2E1H and for 4M3H we find an anharmonicity constant of $\chi_{\alpha/\beta} = -81$ cm^{-1} at 285 K. With $\chi_\delta(285\,\text{K}) \approx -195$ cm^{-1} the impact of hydrogen bonding on the anharmonicity constant is very large in accordance with other findings [23,24,56,57].

3.4. Far-infrared and Raman spectroscopy

Generally, FIR spectroscopy provides access to soft vibrational modes such as the stretching vibration of the hydrogen bridge itself, ν_σ(O···H), for simple alcohols typically found in the 100–200 cm^{-1} wavenumber range [58,59]. Furthermore, in these substances one often finds bending vibrations of the CO group along or perpendicular to the molecular axis [60], δ(CO), at 400–500 cm^{-1}, and librational motions of the hydroxyl group, centered in the ~650 cm^{-1} region [61–64].

In Fig. 7(a) we present FIR spectra of 4M3H and 2E1H in terms of the molar extinction coefficient ε_{IR}. In the absorption spectra of both alcohols there are two broad features discernible, one

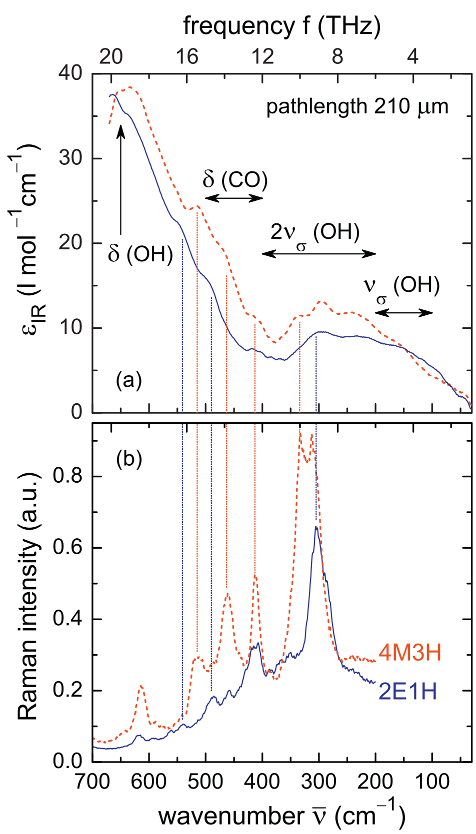

Fig. 7. (a) FIR and (b) low-frequency Raman spectra of 2E1H (solid lines) and 4M3H (dashed lines) recorded at 293 K. The horizontal arrows mark the intervals in which the fundamental and the first overtone of the hydrogen bridge stretching vibration, ν_σ(O···H), as well as bending vibrations of the CO and the OH group, denoted as δ(CO) and δ(OH), respectively, appear in the FIR spectral range. In the Raman spectra, many vibrational features are resolved much better. The vertical dotted lines mark a number of absorption bands that can be found at the same frequency for both experimental methods.

extending from 100 to 380 cm^{-1} and the other from about 400 cm^{-1} to the high-wavenumber end of the spectral range. On top of these features several smaller bands can be identified. We performed additional Raman measurements to confirm these individual peak positions.

In the Raman spectra shown in Fig. 7(b), the prominent background features found in the FIR spectra are not present. For 4M3H there are six peaks (four single and one double peak) in the range from 200 to 660 cm^{-1}. Four of these, at 334, 413, 463, and 515 cm^{-1}, are in accordance with the band positions in the FIR absorption spectrum. The other two bands at 310 and 615 cm^{-1} cannot be seen in the FIR spectrum. For 2E1H five bands can be identified in both the absorption and Raman spectra. These appear at 286, 305, 414, 490, and 541 cm^{-1}.

It is cumbersome to assign any of the Raman bands without proper theoretical calculations. However, the large line width of the background features in the FIR absorption spectra points towards an intermolecular nature of the excited vibrations. Therefore, it is plausible to assign the extinction maximum seen for 4M3H near 650 cm^{-1} to a librational motion of the H-bonded hydroxyl groups, as made for other alcohols [61–64].

Furthermore, the differences in the librational frequencies for the alcohols presently studied provides insight into their supramolecular structure: the 650 cm^{-1} peak seen for 4M3H appears to be shifted towards the blue by about 25 cm^{-1} for 2E1H so that for this latter alcohol only a high-frequency wing rather than a peak is observed. This shift could be explained assuming a ring-like supramolecular structure for 4M3H, rather than a linear one (as for 2E1H), since in 4M3H the hydrogen bonds are expected to be more strained and thus weakened in this configuration.

4. Discussion

The extent to which anharmonicity affects the OH band positions and intensities in the MIR and NIR regions has been debated for a long time [17,23–25,53,56,65]. However, to our knowledge for monohydroxy alcohols it has remained unresolved whether the temperature induced change of the OH overtone absorbance is (i) dominated by a change in the equilibrium of bonded versus non-bonded OH populations or (ii) whether it stems mostly from a temperature dependent anharmonicity. To address this issue let us write the anharmonicity constant, cf. Eq. (1), for the δ band as [23,53]

$$\chi_\delta = -\omega_\delta X_\delta = \omega_\delta \frac{\chi_\delta}{3\overline{\nu}_\delta^{(1)} - \overline{\nu}_\delta^{(2)}}. \tag{2}$$

The above equation defines X as a *dimensionless* anharmonicity constant with reference to the temperature dependent harmonic frequency, $\omega_\delta(T) = 3\overline{\nu}_\delta^{(1)}(T) - \overline{\nu}_\delta^{(2)}(T)$, that can be calculated from the data shown in Fig. 3. The assumption of a simple form for the electrical anharmonicity then allows one to estimate the ratio of the overtone absorbance and the fundamental absorbance as [66,67]

$$\frac{A(\overline{\nu}^{(2)})}{A(\overline{\nu}^{(1)})} = 4X\frac{1-5X}{(1-3X)^2} \approx 4X(1+X). \tag{3}$$

With X typically of the order of only a few percent, an expansion of Eq. (3) essentially yields $4X$. Eq. (3) is plausible since the overtone intensity vanishes in the limit of relative anharmonicities $X \to 0$.

In Fig. 8(a) we present the absorbance ratios for the δ bands of 2E1H and 4M3H, $A_n(\overline{\nu}_\delta^{(2)})/A_n(\overline{\nu}_\delta^{(1)})$ on the right y axis. The index 'n'

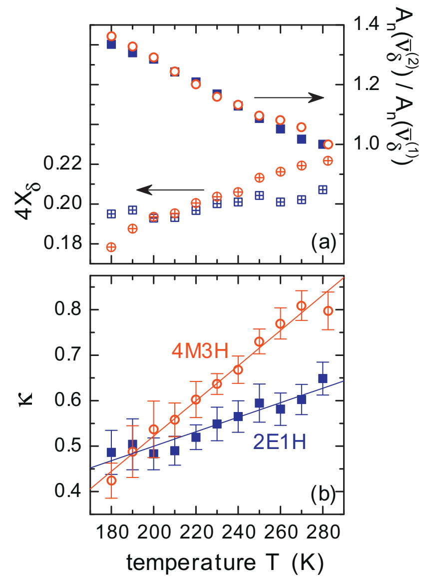

Fig. 8. (a) The left scale presents the anharmonicity term $4X_\delta \approx 4X_\delta(1+X_\delta)$, cf. Eq. (3), and the right scale the ratio of the normalized δ band absorbances for 2E1H and 4M3H. (b) Temperature dependence of the anharmonicity contribution κ. Straight lines are fits to the data. At the highest temperature an average value, T = 282.5 K, was used to represent the 4M3H data.

indicates that the absorbances are normalized by their values at 280 K. In the temperature range covered in Fig. 8 the absorbance ratios of both monohydroxy alcohols increase linearly with decreasing temperature by ~35%. In other words, the thermally induced absorbance gain of the overtone δ band is larger than that of the fundamental one. If the change of the absorbance ratio $A_n(\overline{\nu}_\delta^{(2)})/A_n(\overline{\nu}_\delta^{(1)})$ would mainly stem from an anharmonicity change, then this ratio should show the same temperature trend as X_δ. In Fig. 8(a) we also show the dimensionless anharmonicity, $4X_\delta(1+X_\delta) \approx 4X_\delta$, cf. the left y axis. Here X_δ was calculated using Eq. (2) from the data in Fig. 6(a) and from $\omega_\delta(T)$ as noted just below Eq. (2).

However, Fig. 8(a) reveals that while $A_n(\overline{\nu}_\delta^{(2)})/A_n(\overline{\nu}_\delta^{(1)})$ strongly increases upon cooling, the anharmonicity constants for the δ bands, X_δ, as calculated from Eq. (3) becomes smaller. This decrease of X_δ with decreasing temperature is more pronounced for 4M3H than it is for 2E1H. Thus, the cooling induced absorbance gain of the δ band in the NIR is not dominated by the effective anharmonicity but mainly driven by an increased number of strongly hydrogen bonded OH oscillators.

While referring to anharmonicity effects we rationalized the overtone intensity in terms of the fundamental one. But it remains to be explained why the δ band shifts to the red as the temperature is lowered (see Fig. 3). Is this feature dominated by a gradually increasing cooperativity of the alcohol molecules or rather reflecting changes in anharmonicity? In order to address this question, based on earlier work [53], let us calculate the anharmonicity contribution κ to the red shift as follows: In accord with Eq. (2) the thermally induced change of the δ state's harmonic frequency is $\Delta\omega(T) = \omega_{\alpha/\beta} - \omega_\delta(T)$. Here, $\omega_{\alpha/\beta}$ is the practically temperature independent harmonic frequency of the α/β band (cf. Section 3.3) that is ~3790 cm^{-1} for both samples. The comparison of $\Delta\omega(T)$ with the wavenumber shift of the fundamental δ band position, $\Delta\overline{\nu}^{(1)}(T) = \overline{\nu}_{\alpha/\beta}^{(1)} - \overline{\nu}_\delta^{(1)}(T)$, then yields the relative anharmonicity contribution to the observed red shift of $\overline{\nu}_\delta^{(1)}(T)$ that we define as

$$\kappa(T) = \frac{\Delta\overline{\nu}^{(1)} - \Delta\omega}{\Delta\overline{\nu}^{(1)}}. \tag{4}$$

An anharmonicity contribution of $\kappa = 1$ would imply that the harmonic frequencies of the α/β and of the δ states are equal and that all of the observed red shift is caused by anharmonicity. Conversely, $\kappa = 0$ corresponds to a perfectly harmonic oscillator so that the red shift would entirely stem from cooperativity.

The temperature dependence of κ is presented in Fig. 8(b). Close to room temperature more than 80% of the δ band red shift observed for 4M3H is caused by anharmonicity. This is reasonable because for the sterically hindered monohydroxy alcohol rather strained hydrogen bonds are expected and the prevailing supramolecular structures are small and hence only weakly stabilized by cooperativity effects. Also for 2E1H anharmonicity dominates the red shift at room temperature ($\kappa \sim 65\%$) but with decreasing temperature κ reduces to ∼45% for both samples indicating that cooperativity increases and that larger supramolecular hydrogen bonded clusters develop.

5. Summary

In the current work, previous indications from NIR and Raman spectroscopy [20,40,41] of a “250 K anomaly” are corroborated for 2E1H and 4M3H by the present MIR spectra. Furthermore, the MIR difference spectra allowed us to monitor the thermally induced break-up of the supramolecular structures into alcohol monomers and dimers. From the observation that for 4M3H the peak positions of the δ bands appear always blue shifted with respect to those of 2E1H we concluded that, in general, cooperativity effects are stronger in 2E1H than in 4M3H. This is plausible because for strained hydrogen bonds – as expected to prevail for sterically hindered alcohols such as 4M3H and others [68,69] which form supramolecular rings – such effects should be weaker than for systems like 2E1H which are thought to form chains. In addition, the strained hydrogen bonds in 4M3H cause large anharmonicity. However, toward lower temperatures the anharmonicity decreases, suggestive for ring opening effects as recently hypothesized on the basis of non-linear dielectric spectroscopy [70]. Using a simple approach we calculated the temperature dependent ratio of the NIR and MIR δ band absorbances as a function of anharmonicity and compared it with the experimental peak absorbances. This comparison led us to conclude that a population redistribution rather than anharmonicity effects dominates the increase of the absorbance ratio and hence also the NIR intensity with decreasing temperature. Referring to the harmonic frequency of the δ bands near room temperature, we found that anharmonicity effects dominate the δ band red shift of 4M3H and to a lesser extent also that of 2E1H. With decreasing temperature, though, the impact of cooperativity increases thus reducing the anharmonicity contribution to the red shift of the δ bands. Finally, in the low-wavenumber regime we performed FIR and Raman experiments which hinted at differences in the supramolecular structures of the two monohydroxy alcohols.

Acknowledgment

We thank Peter Lunkenheimer and Jürgen Senker for fruitful discussions. This project was financially supported by the Deutsche Forschungsgemeinschaft under grant no. BO1301/8-2 and by the Cluster of Excellence RESOLV (EXC 1069).

References

[1] W. Kossack, K. Adrjanowicz, M. Tarnacka, W.K. Kipnusu, M. Dulski, E.U. Mapesa, K. Kaminski, S. Pawlus, M. Paluch, F. Kremer, Phys. Chem. Chem. Phys. 15 (2013) 20641.
[2] W. Kossack, W.K. Kipnusu, M. Dulski, K. Adrjanowicz, O. Madejczyk, E. Kaminska, E.U. Mapesa, M. Tress, K. Kaminski, F. Kremer, J. Chem. Phys. 140 (2014) 215101.
[3] K. Adrjanowicz, K. Kaminski, M. Dulski, P. Wlodarczyk, G. Bartkowiak, L. Popenda, S. Jurga, J. Kujawski, J. Kruk, M.K. Bernard, M. Paluch, J. Chem. Phys. 139 (2013) 111103.
[4] M.A. Czarnecki, Appl. Spectrosc. Rev. 46 (2011) 103.
[5] P. Sassi, F. Palombo, R.S. Cataliotti, M. Paolantoni, A. Morresi, J. Phys. Chem. A 111 (2007) 6020.
[6] A.V. Iogansen, Spectrochim. Acta A 55 (1999) 1585.
[7] P. Papadopoulos, W. Kossack, F. Kremer, Soft Matter 9 (2013) 1600.
[8] W.K. Kipnusu, W. Kossack, C. Iacob, P. Zeigermann, M. Jasiurkowska, J.R. Sangoro, R. Valiullina, F. Kremer, Soft Matter 9 (2013) 4681.
[9] A. Karpfen, Adv. Chem. Phys. 123 (2002) 469.
[10] J.P. Perchard, Z. Mielke, Chem. Phys. 264 (2001) 221.
[11] F. Kollipost, K. Papendorf, Y.-F. Lee, Y.-P. Lee, M.A. Suhm, Phys. Chem. Chem. Phys. 16 (2014) 15948.
[12] M. Tomšič, A. Jamnik, G.F. Popovski, O. Glatter, L. Vlček, J. Phys. Chem. B 111 (2007) 1738.
[13] C. Gainaru, S. Kastner, F. Mayr, P. Lunkenheimer, S. Schildmann, H.J. Weber, W. Hiller, A. Loidl, R. Böhmer, Phys. Rev. Lett. 107 (2011) 118304.
[14] S. Schildmann, A. Reiser, R. Gainaru, C. Gainaru, R. Böhmer, J. Chem. Phys. 135 (2011) 174511.
[15] L.P. Singh, R. Richert, Phys. Rev. Lett. 109 (2012) 167802.
[16] C. Gainaru, R. Figuli, T. Hecksher, B. Jakobsen, J.C. Dyre, M. Wilhelm, R. Böhmer, Phys. Rev. Lett. 112 (2014) 098301.
[17] C. Boudéron, J.J. Péron, C. Sandorfy, J. Phys. Chem. 76 (1972) 864.
[18] S.K. Stephenson, R.D. Offeman, G.H. Robertson, W.J. Orts, Chem. Eng. Sci. 62 (2007) 3019.
[19] S. Bauer, H. Wittkamp, S. Schildmann, M. Frey, W. Hiller, T. Hecksher, N.B. Olsen, C. Gainaru, R. Böhmer, J. Chem. Phys. 139 (2013) 134503.
[20] S. Bauer, K. Burlafinger, C. Gainaru, P. Lunkenheimer, W. Hiller, A. Loidl, R. Böhmer, J. Chem. Phys. 138 (2013) 094505.
[21] L.A. Woodward, Introduction to the Theory of Molecular Vibrations and Vibrational Spectroscopy, Clarendon Press, Oxford, 1972.
[22] A.B. McCoy, J. Phys. Chem. B 118 (2014) 8286.
[23] P. Schuster, G. Zundel, C. Sandorfy, The Hydrogen Bond II: Structure and Spectroscopy, North-Holland Publishing Company, Amsterdam, 1976.
[24] U. John, K.P.R. Nair, Spectrochim. Acta A 61 (2005) 2555.
[25] C. Sandorfy, J. Mol. Struct. 790 (2006) 50.
[26] M. Morita, K. Takahashi, Phys. Chem. Chem. Phys. 15 (2013) 114.
[27] T. Fukasawa, T. Sato, J. Watanabe, Y. Hama, W. Kunz, R. Buchner, Phys. Rev. Lett. 95 (2005) 197802.
[28] R. Nozaki, AIP Conf. Proc. 1518 (2013) 276.
[29] U. Møller, D.G. Cooke, K. Tanaka, P.U. Jepsen, J. Opt. Soc. Am. B 26 (2009) A113.
[30] J.K. Vij, C.J. Reid, Chem. Phys. Lett. 92 (1982) 528.
[31] J.K. Vij, C.J. Reid, M.W. Evans, Mol. Phys. 50 (1983) 935.
[32] B. Stuart, Infrared Spectroscopy: Fundamentals and Applications, Wiley, Chichester, 2004.
[33] J.M. Chalmers, P.R. Grifftiths, Handbook of Vibrational Spectroscopy 3, Wiley, Chichester, 2002.
[34] M. Paolantoni, P. Sassi, A. Morresi, R.S. Cataliotti, Chem. Phys. 310 (2005) 169.
[35] S.J. Barlow, G.V. Bondarenko, Y.E. Gorbaty, T. Yamaguchi, M. Poliakoff, J. Phys. Chem. A 106 (2002) 10452.
[36] J.M. Andanson, J.C. Soetens, T. Tassaing, M. Besnard, J. Chem. Phys. 122 (2005) 174512.
[37] H. Graener, T.Q. Ye, A. Laubereau, J. Chem. Phys. 90 (1989) 3413.
[38] F. Palombo, T. Tassaing, Y. Danten, M. Besnard, J. Chem. Phys. 125 (2006) 094503.
[39] M.A. Czarnecki, D. Wojtków, K. Haufa, Chem. Phys. Lett. 431 (2006) 294.
[40] S. Bauer, K. Moch, P. Münzner, S. Schildmann, C. Gainaru, R. Böhmer, J. Non-Cryst. Solids 407 (2015) 384.
[41] A. Hédoux, Y. Guinet, L. Paccou, P. Derollez, F. Danède, J. Chem. Phys. 138 (2013) 214506.
[42] W. Dannhauser, J. Chem. Phys. 48 (1968) 1911.
[43] S.P. Bierwirth, T. Büning, C. Gainaru, C. Sternemann, M. Tolan, R. Böhmer, Phys. Rev. E 90 (2014) 052807.
[44] P. Sillrén, J. Bielecki, J. Mattson, L. Börjesson, A. Matic, J. Chem. Phys. 136 (2012) 094514.
[45] W.A.P. Luck, W. Ditter, J. Mol. Struct. 1 (1967–1968) 261.
[46] N. Michniewicz, M.A. Czarnecki, J.P. Hawranek, J. Mol. Struct. 844–845 (2007) 181.
[47] M.A. Czarnecki, K. Orzechowski, J. Phys. Chem. A 107 (2003) 1119.
[48] M.A. Czarnecki, H. Maeda, Y. Ozaki, M. Suzuki, M. Iwahashi, J. Phys. Chem. A 102 (1998) 9117.
[49] M.A. Czarnecki, J. Phys. Chem. A 104 (2000) 6356.
[50] K. Ohno, T. Shimoaka, N. Akai, Y. Katsumoto, J. Phys. Chem. A 112 (2008) 7342.
[51] M.A. Czarnecki, M. Czarnecka, Y. Liu, Y. Ozaki, M. Suzuki, M. Iwahishi, Spectrochim. Acta A 51 (1995) 1005.
[52] G.E. Walrafen, M.R. Fisher, M.S. Hokmabadi, W.H. Yang, J. Chem. Phys. 85 (1986) 6970.
[53] M. Asselin, C. Sandorfy, J. Mol. Struct. 8 (1971) 145.
[54] R.B. Gupta, R.L. Brinkley, AIChE J. 44 (1998) 207.
[55] G. Herzberg, Molecular Spectra and Molecular Structure: II – Infrared and Raman Spectra of Polyatomic Molecules, Van Nostrand, New York, 1964.

[56] G. Durocher, C. Sandorfy, J. Mol. Spectrosc. 15 (1965) 22.
[57] C. Sandorfy, J. Mol. Struct. 614 (2002) 365.
[58] K.D. Möller, W.G. Rothschild, Far-Infrared Spectroscopy, Wiley, New York, 1971.
[59] R.F. Lake, H.W. Thompson, Proc. R. Soc. Lond. A 291 (1966) 469.
[60] S. Krimm, Fortschr. Hochpolym. Forsch. 2 (1960) 51.
[61] M.S. Skaf, T. Fonseca, B.M. Ladanyi, J. Chem. Phys. 98 (1993) 8929.
[62] S.M. Vechi, M.S. Skaf, J. Chem. Phys. 123 (2005) 154507.
[63] R.W. Larsen, M.A. Suhm, J. Chem. Phys. 125 (2006) 154314.
[64] R.W. Larsen, M.A. Suhm, Phys. Chem. Chem. Phys. 12 (2010) 8152.
[65] T. Di Paolo, C. Bourdéron, C. Sandorfy, Can. J. Chem. 50 (1972) 3161.
[66] W. Groh, Makromol. Chem. 189 (1988) 2861.
[67] R. Böhmer, C. Gainaru, R. Richert, Phys. Rep. 545 (2014) 125.
[68] M. Huelsekopf, R. Ludwig, J. Mol. Liq. 98–99 (2002) 163.
[69] H. Weingärtner, H. Nadolny, A. Oleinikova, R. Ludwig, J. Chem. Phys. 120 (2004) 11692.
[70] L.P. Singh, C. Alba-Simionesco, R. Richert, J. Chem. Phys. 139 (2013) 144503.